A circumferentially flanged tibial tray minimizes bone–tray shear micromotion

D S Barker[1]*, **K E Tanner**[1,2], and **L Ryd**[3]
[1]Department of Orthopaedics, Lund University Hospital, Lund, Sweden
[2]Department of Materials, Queen Mary University of London, London, UK
[3]Department of Orthopaedics, Karolinska University Hospital, Stockholm, Sweden

The manuscript was received on 27 June 2003 and was accepted after revision for publication on 6 July 2005.

DOI: 10.1243/095441105X34464

Abstract: Aseptic loosening of the tibial component is the major complication of total knee arthroplasty. There is an association between early excessive shear micromotion between the bone and the tray of the tibial component and late aseptic loosening. Using non-linear finite element analysis, whether a tibial tray with a circumferentially flanged rim and a mating cut in the proximal tibia could minimize bone–tray shear micromotion was considered. fifteen competing tray designs with various degrees of flange curvature were assessed with the aim of minimizing bone–tray shear micromotion. A trade-off was found between reducing micromotion and increasing peripheral cancellous bone stresses. It was found that, within the limitations of the study, there was a theoretical design that could virtually eliminate micromotion due to axial loads, with minimal bone removal and without the use of screws or pegs.

Keywords: total knee replacement, micromotion, prosthesis design, stress shielding, non-cemented

1 INTRODUCTION

The main cause of failure of total knee replacement (TKR) is aseptic loosening, with the tibial component implicated in a large proportion of these failures [**1**]. The aetiology of this loosening is unclear; however, both mechanical and biological factors have been implicated [**2–4**]. Following non-cemented TKR, there is a dead zone of cancellous bone under the tibial tray. During the early post-operative phase, weight bearing and gait will cause frictional slip, or shear micromotion, between the tibial tray and the underlying bone. This movement is partly due to the large difference between the radial stiffnesses of metal and cancellous bone combined with negligible mechanical strength of the interface. The magnitude of this early shear micromotion will influence the long-term tissue type and hence fixation between the tray and bone. There is strong evidence that excessive initial shear micromotion (greater than 50 μm) between a metal implant and bone is detrimental to long-term implant function and stability [**5–13**]. A further hypothesis for tibial tray loosening has been overloading of the subtray cancellous bone [**14**]. There is undoubtedly a relationship between shear micromotion and load transfer to the proximal tibia and a combination of these factors is likely to influence subtray tissue differentiation and the ultimate success of long-term tray fixation.

Several investigators have studied the non-cemented tibial tray in relation to reducing shear micromotion and promoting physiological load transfer [**15–24**]. Tibial component features that were examined included central keels, offset pegs and screws, different materials and geometry, metal backing, and surface finish. Various design features were recommended on the basis of these analyses. Each of the aforementioned studies considered tray designs that were flat in the transverse plane. Shrivastava *et al.* [**25**] showed that a tibial tray that was cemented and had a full 'dome' shape could reduce and more evenly distribute cement stresses.

* *Corresponding author: Portland Orthopaedics Limited, Unit 3/44, McCauley Street, Matraville, NSW 2036, Australia. email: d.barker@portland-orthopaedics.com*

This theoretical tray was designed to lie on a flat cancellous bone surface with bone cement acting as an intermediary layer. Similarly, Vasu *et al.* [**26**] described a special shape of tibial component to minimize bone–tray interface stresses.

It has been shown that shear micromotion between the tray and bone and the presence of fibrous tissue are both greatest at the periphery [**20**, **27**]. Investigations were carried out to determine whether a non-cemented tibial tray incorporating a circumferential flange could reduce post-operative bone–tray shear micromotion.

There were two principal aims of this study. The first aim was to determine, by parametrically varying the curvature of the flange, whether there was an optimum tray shape that could theoretically eliminate bone–tray shear micromotion. The second aim was to assess the subtray cancellous bone stresses for different flange shapes and to determine whether there was a relationship between the bone stresses and shear micromotion. Finite element (FE) analysis was utilized for this undertaking.

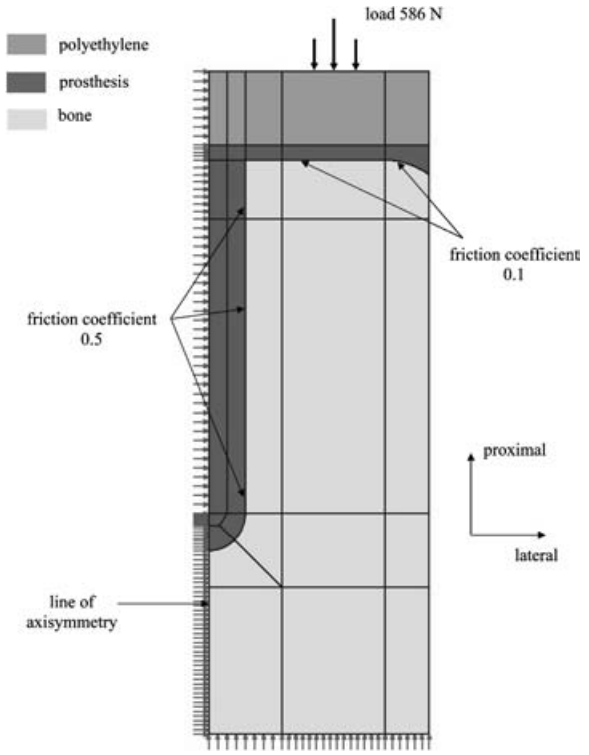

Fig. 1 Schematic diagram of prosthetic tibial geometry showing the *p*6*q*2 tray design

2 MATERIALS AND METHODS

A simplified axisymmetric FE model of a prosthetic tibia was created. The LUSAS FE program was used for all the preprocessing, post-processing, and actual processing (FEA Pty Ltd, Surrey, UK). The two-dimensional geometric surfaces used to define the axisymmetric mesh of the proximal tibia are shown in Fig. 1. The geometry was a simplified coronal plane representation of a metal-backed tibial implant inserted into the proximal tibia.

2.1 Geometry

The radius of the proximal tibial tray was assumed to be 30 mm. The thickness of the tibial tray was 2 mm and was covered with 10 mm of polyethylene. The length of the tibial post was 50 mm with a radius of 5 mm. The total height of the model was 90 mm. The various design parameters of the tibial tray are detailed below.

2.2 Tibial tray flange shape

Sixteen different tibial plateau shapes were considered: a tray that was completely flat and 15 designs incorporating circumferential flanges. Each tray design consisted of a flat region and a parabolic region and the design was designated *piqj*, where *i* represented the radial distance from the subtray peripheral bone at which the parabolic bone cut was made and *j* represented the vertical distance from the subtray peripheral bone at which the parabolic cut intersected with the peripheral boundary of bone. The *p* axis was equivalent to the radial axis in the transverse plane and the *q* axis was equivalent to the proximodistal axis. For each of $i = 2$, 4, 6, 8, and 10, three values of $j = 2$, 4, and 6 were considered, giving 15 tray designs incorporating a circumferential flange. Two examples are shown in Fig. 2. For each parabola, the condition was imposed such that the slope of the tangent at the point $p = i$ was 0. Thus, two points and the condition $\mathrm{d}q/\mathrm{d}p(i) = 0$ were known, which allowed a unique parabola to be defined in *pq* space. The parabolic curves were imported into the FE model using cubic splines.

2.3 Loading

The magnitude of applied load was calculated by assuming an average vertical cancellous bone stress of 1.34 MPa under the tibial tray [**2**]. This stress level meant that a total load of 586 N was applied in the vertical direction with the centroid of load acting through a point 10 mm inside the lateral edge of the tibia (Fig. 1). The radial load distribution was assumed to be 2.5 mm wide with a triangular

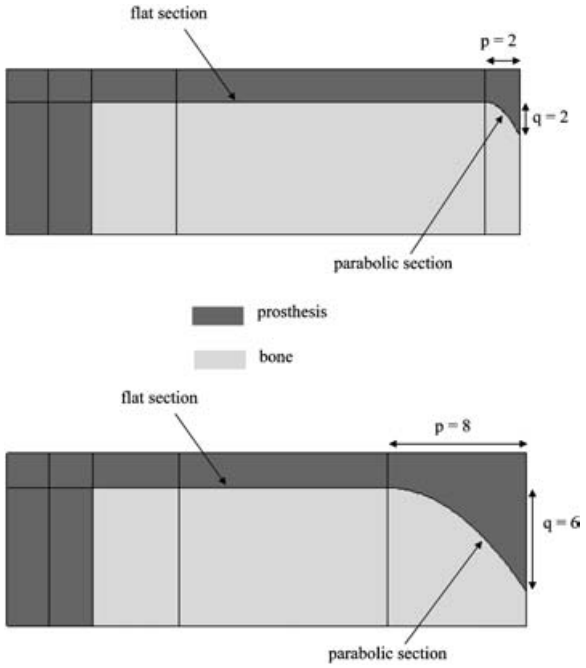

Fig. 2 Illustrations of the *p*2*q*2 (top) and *p*8*q*6 (bottom) designs

distribution. The use of an axisymmetric model meant that the load was applied through 2π rad. Lateral loading was not considered in this study.

2.4 Restraints

The distal bone nodes were fully restrained in the proximodistal direction and the nodes lying on the line of axisymmetry were restrained in the mediolateral direction only (Fig. 1).

2.5 Materials

Three materials were considered (Fig. 1):

(a) prosthesis, $E = 200\,000$ MPa, $\nu = 0.3$;
(b) cancellous bone, $E = 300$ MPa, $\nu = 0.3$;
(c) polyethylene, $E = 1000$ MPa, $\nu = 0.3$.

Non-linear, heterogeneous, anisotropic, or time-dependent material properties were not considered. The epiphyseal region of the proximal tibia contains a paucity of cortical bone and thus was not included in this simplified model.

2.6 Interface conditions

The vertical post was allowed to slip relative to the surrounding bone using a Coulomb friction model with a representative coefficient of friction of 0.5 for all analyses (Fig. 1). This value contained uncertainty and was subjected to a sensitivity analysis (range 0.2–0.7). Variation in this post-bone friction coefficient had a small quantitative effect on the results presented in this study but did not alter the conclusions of the study.

The interface between the tibial tray and underlying bone was modelled with Coulomb friction with a coefficient of friction of 0.1 (Fig. 1). It has been shown that the use of Coulomb friction may underestimate the magnitude of micromotion at a tray–bone interface [**28**]. To take this into account, a lower than usual friction coefficient was used to model the interface between tray and bone. The friction coefficient of 0.1 used as the immediate post-operative condition will produce more realistic levels of micromotion, compared with the experimentally measured value of 0.7, which was intended for use in a non-linear friction law. The lower value used in this study was also chosen to illustrate a worst case for micromotion and should be used with caution in other studies.

2.7 Mesh

Predominantly four-node quadrilateral axisymmetric elements were created from the geometric model shown in Fig. 1. A small number of three-node triangular elements were used to prevent aspect ratio errors. Enhanced strain elements were used to improve performance in bending by greatly reducing parasitic shear. Convergence tests were performed to ensure the models had sufficient precision. A typical non-linear analysis consisted of approximately 4200 elements and 4500 nodes.

2.8 Output

For each of the 16 tray designs, the maximum shear micromotion between the tray and bone was considered, as well as patterns and magnitudes of the compressive stresses in the subtray cancellous bone. The tibial tray design that produced the lowest shear micromotion was designated the optimum design.

2.9 Three-dimensional validation study

An axisymmetric FE analysis assumes that the loads applied through the knee joint have a uniform circumferential distribution. In reality, knee joint loads act through the medial and lateral condyles. It was considered necessary to verify whether an axisymmetric FE model was suitable for optimizing the tibial tray design with the aim of minimizing bone–tray shear micromotion. To achieve this, two fully three-dimensional FE models were created by sweeping the two-dimensional geometry, for both the traditional flat tray design and the optimum

design, through 90° about the centre-line of the tibia. It was unnecessary to revolve the surfaces through 360° because of the assumed loading and geometric symmetry about the coronal and sagittal planes, and only one-quarter of the proximal tibia was required. The resultant volumes were subsequently meshed with eight-node brick elements. These elements also used a modified strain formulation to improve their behaviour in bending. The total knee joint load was assumed to be distributed equally between the medial and lateral condyles. Furthermore, each condylar loading patch was described by a 60° arc with a radial thickness of 2.5 mm and was symmetrical about the coronal plane, thus producing load in the tibial plateaux only. As for the axisymmetric study, the centroid of the load was assumed to act through a point 10 mm inside the lateral edge of the tibia. The total load applied through each condyle was calculated by multiplying the axisymmetric load of 586 N by 2π and dividing by two. The model was therefore loaded in a more realistic manner corresponding to medial and lateral condyle weight bearing. This model contained approximately 9300 nodes and 7750 elements.

3 RESULTS

The peak shear micromotions between tray and bone for each of the 16 tray shapes are presented in Fig. 3. A positive micromotion indicated that the tray displaced further than the bone and a negative micromotion indicated that there was greater bone movement than tray. For a traditional flat design, there was a relatively large (23 μm) lateral expansion of bone relative to the tray. This was due to Poisson expansion of the bone with its considerably lower stiffness than the apposing tray. For the relatively tightly 'capped' *p*2*q*6 design with sharp flange curvature, the relative motion was reversed with the near-vertical flange of the tray moving 37 μm more than the bone. It can be seen that, for designs *p*6*q*2 and *p*8*q*2, shear micromotion was virtually eliminated. The results also showed that there was more than one design solution for eliminating bone–tray shear micromotion. The trend for the *q*4 designs implied that, for a *p* value of 12–14 mm, zero micromotion could be achieved. This was, however, at the expense of greater bone removal.

Contour plots of the peak compressive stresses in the bone underlying the tibial tray for flat *p*2*q*6 ('capped') and *p*6*q*2 ('optimum') designs are shown in Fig. 4. A compressive stress concentration was noted at the extreme lateral periphery of bone for each tray. The magnitude of this peak stress concentration increased across all design types as the shear micromotion decreased. A summary of the peak principal compressive cancellous bone stresses is presented in Table 1.

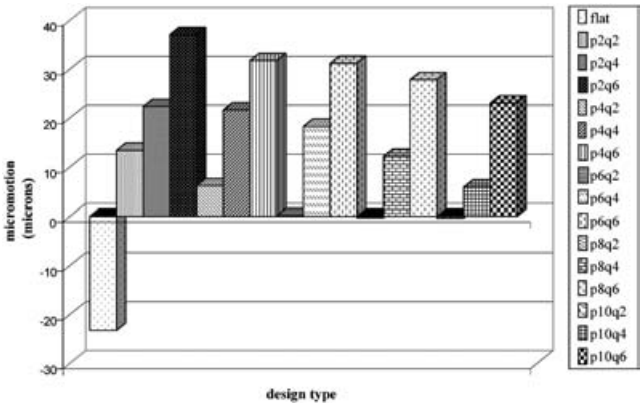

Fig. 3 Peak shear micromotion between tibial tray and bone

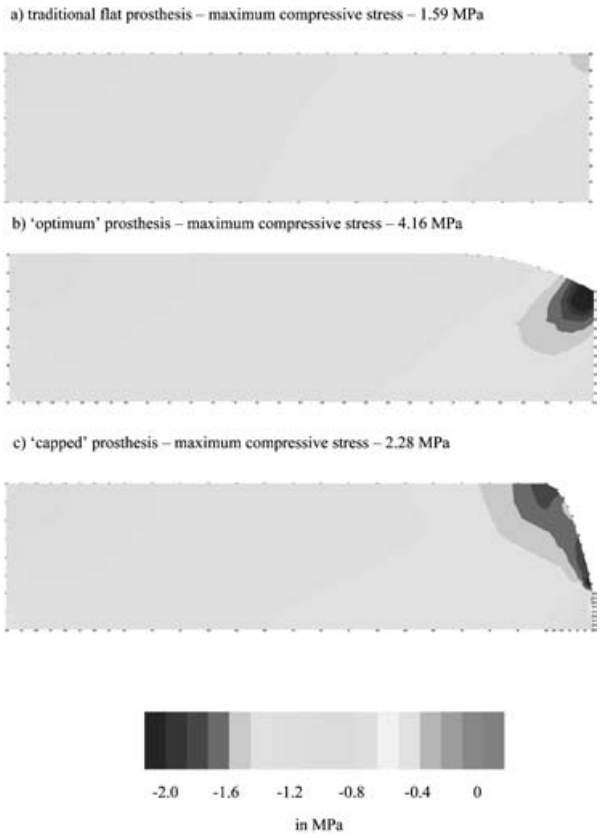

Fig. 4 Peak subtray bone compressive stress contour plot for (a) the traditional flat tray, (b) the 'optimum' design, and (c) the 'capped' design. The right-hand boundary represents the lateral edge of bone. The upper boundary represents the bone–tray boundary. The left boundary represents the post-bone boundary

Table 1 Peak compressive bone stresses for three tibial tray designs

	Peak compressive bone stresses (MPa)		
	Flat	Optimum	Capped
Under loading point	1.33	1.24	1.31
Peripheral	1.59	4.16	2.28

Considering the three-dimensional model, the redistribution of stresses in the coronal plane and the pattern of micromotion in the coronal plane for the intact and prosthetic strains were identical to those of the axisymmetric models. The magnitudes of compressive stresses as well as bone–tray shear micromotion were increased by up to 120 per cent in the coronal plane and reduced by up to 90 per cent in the sagittal plane, compared with the axisymmetric analysis. Importantly, the optimized *p*6*q*2 design eliminated bone–tray shear micromotion in the coronal plane of the three-dimensional model, whereas 51 μm of motion was predicted for a flat tray design considering the three-dimensional model.

4 DISCUSSION

A fundamental objective of non-cemented TKR design is to minimize early shear micromotion and thus to promote bone ingrowth. This is the first time to the present authors' knowledge that the possible use of a tibial tray with a circumferential flange has been considered in tibial tray design. It was found that, for a modest increase in bone removal, only 2 mm in the vertical direction, bone–tray shear micromotion could theoretically be reduced to zero for symmetric axial loading. This was due to a cross-over effect between the relative motion of the tray and bone, when flat and 'capped' designs were considered. The traditional flat design induced greater bone than tray movement in a radial direction. A 'capped' design such as *p*2*q*6, where there was a sharp bend between the horizontal and vertical components, induced greater tray than bone movement in a more vertical direction. Between these two extremes, there is a design that theoretically will induce zero shear micromotion under symmetric axial loads. The elimination of bone–tray shear micromotion was, however, at the expense of a stress concentration at the lateral periphery.

Several other studies have compared tibial implant designs with subtray cancellous bone stresses as the outcome of interest [**14**, **16**, **18**, **20**, **22**, **25**, **29–32**]. A comparison of results is difficult owing to the variety of assumptions made in each model, including the load and boundary conditions, the material properties, the inclusion of cement, the tibial prosthesis design, and the role of the epiphyseal shell. Vasu *et al.* [**16**], Garg and Walker [**15**], and Shrivastava *et al.* [**25**] compared intact and prosthetic strains. Vasu *et al.* [**16**] demonstrated that a metal-backed non-cemented tibial tray with a central post caused a reduction in proximal compressive cancellous bone stresses; i.e. there was underloading of the subtray bone. Garg and Walker [**15**] found that the peak compressive cancellous bone stress was directly under the centroidal point of loading for the intact tibia, and that the peak stress following implantation of a metal-backed tibial prosthesis was greatly reduced with a more even stress distribution. Shrivastava *et al.* [**25**] stated that 'the shell action of a domed prosthesis results in a transfer of a major part of the load from the central portion of the prosthesis to its edges'. It should be noted that these investigators considered a cemented fully domed tray. These findings complement the results reported by the present authors, which illustrated stress concentrations at the periphery when considering a non-cemented tibial tray with a central post.

Quantitatively, Garg and Walker [**15**] found subtray compressive cancellous bone stresses of approximately 3.5 MPa under the loading point. Vasu *et al.* [**16**] found peak stresses of approximately 2.0 MPa for both the intact and the prosthetic tibia. Similarly, Taylor *et al.* [**14**] reported peak stresses of approximately 2.0 MPa. Hashemi and Shirai-Adl [**20**] found peak stresses of approximately 3.0 MPa. Dawson and Bartel [**18**], using an axisymmetric FE model, found peak stresses of approximately 3.0 MPa. The present authors found peak bone stresses of 1.33 MPa under the loading point and 1.59 MPa at the lateral periphery for the flat tray.

Comparing micromotion data reported in similar studies, Shirazi-Adl and Ahmed [**21**] reported a peak bone–tray shear micromotion of 13.2 μm (loading scaled to 2000 N) for a frictionless bone–tray interface. Hashemi and Shirazi-Adl [**20**] reported a peak bone–tray shear micromotion of approximately 15 μm. Rakotomanana *et al.* [**22**] reported peak bone–tray shear micromotions of approximately 50 μm for a non-cemented tibial tray. The same workers reported subtray compressive cancellous bone stresses of 8.1 MPa. These very high values lead to questions concerning the precision of the model, considering that only 130 plane strain elements were used. The present authors found a peak bone–tray shear micromotion of 23 μm for a flat tibial tray.

The similarity of the results obtained by the present authors to other model data from the literature adds credence to the use of the simplified model. It is still important to interpret the data in the light of the limitations and assumptions of the present FE modelling approach. The limitations and assumptions include the following.

1. An axisymmetric model was constructed that considered circumferential bone stiffness but did not take into account the varying circumferential three-dimensional loading distribution of the proximal tibia. It was felt that a simple two-dimensional plane stress–strain analysis would be non-realistic, neglecting the important role of circumferential stiffness. To reduce excessive computational expense, two-dimensional geometry was chosen with axisymmetric elements to provide a more accurate representation of the actual situation. It was found when considering a simplistic three-dimensional model that patterns of bone–tray shear micromotion reduction were the same in the coronal plane and that an axisymmetric approach was reasonable for the objectives of the study. The size of the loading arc (60°) in the three-dimensional model may have slightly biased the three-dimensional data towards the axisymmetric data.
2. The bone was considered to be linear, homogeneous, and isotropic, whereas, in reality, proximal tibial cancellous bone has non-linear, time-varying, heterogeneous, and anisotropic material properties. The use of an isotropic material model will overestimate the cancellous bone stresses and underestimate the bone–tray shear micromotion [**22**]. A homogeneous material model will also alter the magnitude of stresses and micromotions. The role of the metaphyseal shell is also controversial. There is a debate in the literature about whether this shell has a substantial mechanical contribution or whether it can be neglected. The best evidence implies that the metaphyseal shell does not bear a large percentage of the axial load and is negligible in proximal tibial mechanics [**15**, **33**, **34**]. The modelling of the proximal tibia without a cortical bone shell also provided a worst-case scenario for micromotion and cancellous bone loading.
3. Complete and continuous contact between the tibial tray and subtray cancellous bone was assumed. In reality, contact may be limited to discrete regions along the interface, leading to overstressing at some locations and understressing at others [**15**].
4. The importance of two mathematical parameters in modelling contact problems in FE analysis, namely interface stiffness and convergence tolerance, has been emphasized [**35**]. Model limits on these parameters were established and reviewed. The convergence criterion chosen was the 'residual force norm'. This parameter is the sum of the squares of all the residual forces as a percentage of the sum of the squares of all the external forces. Initially a tight value of 0.1 was chosen. Increasing interface stiffness between the tray and bone decreased deleterious node co-penetrations (when tray nodes penetrated the bone surface) but increased interface 'chatter' (numerical oscillation) which significantly increased computation time and often disallowed a solution. A trade-off was required between 'slackening' the convergence tolerance to allow a solution and increasing the interface stiffness to minimize co-penetrations. A residual force norm of 1.0 was chosen, with the interface stiffness chosen such that co-penetrations did not affect the results by more than 5 per cent.
5. Load transfer across the knee joint during particular activities *in vivo* will lead to shear or transverse loads being applied to the tibial tray. The extent to which the introduction of a circumferential flange would prevent the subsequent micromotions induced by shear loading is unclear. These potential effects require further consideration.

These limitations are reasonable when considering the objectives of the study, which were to investigate the efficacy of a tibial tray with a circumferential flange and to optimize the design such that shear micromotion due to predominant axial loads would be minimized. It is doubtful whether the inclusion of more sophisticated material and geometric models would alter the qualitative findings that incorporating a circumferential flange into the tibial tray design will reduce micromotion but increase peripheral compressive stresses compared with a traditional flat design. Furthermore, model properties were the same throughout all analyses, so any errors would be systematic.

The clinical implications of excess metal–bone micromotion are now well established. The early stability of the metal–bone interface, and hence the long-term implant survival, is dependent on the amount of relative micromotion. The clinical implications of subtray compressive cancellous bone stresses remain unclear. There appears to be a window of stress in the proximal cancellous bone

that will enable homeostasis. Taylor *et al.* [**14**] suggested that component migration was related to cancellous bone fatigue failure due to overloading. However, there was no comparison of prosthetic and intact tibial cancellous bone stresses, so it was not possible to determine whether the prosthesis designs considered in their study increased or decreased cancellous bone stresses relative to intact conditions. In contradistinction, it has been suggested that underloading of regions of subtray cancellous bone can lead to bone resorption and subsidence [**16**]. The state of stress in the subtray cancellous bone and its relationship to subsidence and loosening need further investigation.

The axisymmetric model used in this study implies a uniform circumferential distribution of bone–tray shear micromotion. The three-dimensional analysis demonstrated that, when considering bicondylar loading, micromotions in the sagittal plane were greatly reduced in comparison with the coronal plane. This has implications for the three-dimensional design of a tibial tray with a circumferential flange. It may be that the tray only requires a flange within a particular range of angle sweeping circumferentially from the coronal plane. Fully three-dimensional analyses will clarify this aspect of design, which will also depend on the ease of manufacturing tools to provide for the mating tibial cut. Furthermore, three-dimensional analyses will enable an assessment of the extent to which a circumferential flange can prevent excessive micromotion due to lateral loads.

In summary, it has been found that, by incorporating a circumferential flange into tibial tray design, a theoretical condition of zero bone–tray shear micromotion is possible for axial loads. It has also been found that a *p*6*q*2 design, i.e. a design where the curve starts 6 mm from the bone edge and drops by 2 mm, was optimal in reducing bone–tray shear micromotion, and this design involved only a small increase in bone removal. A trade-off was identified between decreasing shear micromotion and increasing peripheral compressive cancellous bone stress. Importantly, neither a flat nor a 'capped' tibial tray is ideal for minimizing bone–tray shear micromotion. The concept of a circumferential flange deserves further attention in tibial tray design.

ACKNOWLEDGEMENT

This work was partially supported through a grant from DePuy, Inc.

REFERENCES

1 **Robertsson, O., Knutson, K., Lewold, S.,** and **Lidgren, L.** The Swedish Knee Arthroplasty Register 1975–1997: an update with special emphasis on 41,223 knees operated on in 1988. *Acta Orthop. Scand.*, 2001, **72**, 503–513.

2 **Giori, N. J., Ryd, L.,** and **Carter, D. R.** Mechanical influences on tissue differentiation at bone–cement interfaces. *J. Arthroplasty*, 1995, **10**, 514–522.

3 **Bauer, T. W.** and **Schils, J.** The pathology of total joint arthroplasty. I. Mechanisms of implant fixation. *Skeletal Radiol.*, 1999, **28**, 423–432.

4 **Aspenberg, P.** and **Herbertsson, P.** Periprosthetic bone resorption. Particles versus movement. *J. Bone Jt Surg.*, 1996, **78B**, 641–646.

5 **al Saffar, N.** The osteogenic properties of the interface membrane at the site of orthopedic implants: the impact of underlying joint disease. *J. Long-term Effects Med. Implants*, 1999, **9**, 23–45.

6 **Ramamurti, B. S., Orr, T. E., Bragdon, C. R., Lowenstein, J. D., Jasty, M.,** and **Harris, W. H.** Factors influencing stability at the interface between a porous surface and cancellous bone: a finite element analysis of a canine *in vivo* micromotion experiment. *J. Biomed. Mater. Res.*, 1997, **36**, 274–280.

7 **Fukuoka, S., Yoshida, K.,** and **Yamano, Y.** Estimation of the migration of tibial components in total knee arthroplasty. A Roentgen stereophotogrammetric analysis. *J. Bone Jt Surg.*, 2000, **82B**, 222–227.

8 **Bragdon, C. R., Burke, D., Lowenstein, J. D., O'Connor, D. O., Ramamurti, B., Jasty, M.,** and **Harris, W. H.** Differences in stiffness of the interface between a cementless porous implant and cancellous bone *in vivo* in dogs due to varying amounts of implant motion. *J. Arthroplasty*, 1996, **11**, 945–951.

9 **Jasty, M., Bragdon, C., Burke, D., O'Connor, D., Lowenstein, J.,** and **Harris, W. H.** *In vivo* skeletal responses to porous-surfaced implants subjected to small induced motions. *J. Bone Jt Surg.*, 1997, **79A**, 707–714.

10 **Goodman, S. B.** The effects of micromotion and particulate materials on tissue differentiation. Bone chamber studies in rabbits. *Acta Orthop. Scand., Suppl.*, 1994, **258**, 1–43.

11 **Pilliar, R. M., Lee, J. M.,** and **Maniatopoulos, C.** Observations on the effect of movement on bone ingrowth into porous-surfaced implants. *Clin. Orthop.*, 1986, **208**, 108–113.

12 **Ryd, L., Albrektsson, B. E., Carlsson, L., Dansgard, F., Herberts, P., Lindstrand, A., Regner, L.,** and **Toksvig-Larsen, S.** Roentgen stereophotogrammetric analysis as a predictor of mechanical loosening of knee prostheses. *J. Bone Jt Surg.*, 1995, **77B**, 377–383.

13 **Grewal, R., Rimmer, M. G.,** and **Freeman, M. A.** Early migration of prostheses related to long-term survivorship. Comparison of tibial components in knee replacement. *J. Bone Jt Surg.*, 1992, **74B**, 239–242.

14 **Taylor, M., Tanner, K. E.,** and **Freeman, M. A. R.** Finite element analysis of the implanted proximal tibia: a relationship between the initial cancellous bone stresses and implant migration. *J. Biomechanics*, 1998, **31**, 303–310.

15 **Garg, A.** and **Walker, P. S.** The effect of the interface on the bone stresses beneath tibial components. *J. Biomechanics*, 1986, **19**, 957–967.

16 **Vasu, R., Carter, D. R., Schurman, D. J.,** and **Beaupre, G. S.** Epiphyseal-based designs for tibial plateau components. 1: stress analysis in the frontal plane. *J. Biomechanics*, 1986, **19**, 647–662.

17 **Sumner, D. R., Berzins, A., Turner, T. M., Igloria, R.,** and **Natarajan, R. N.** Initial *in vitro* stability of the tibial component in a canine model of cementless total knee replacement. *J. Biomechanics*, 1994, **27**, 929–939.

18 **Dawson, J. M.** and **Bartel, D. L.** Consequences of an interference fit on the fixation of porous-coated tibial components in total knee replacement. *J. Bone Jt Surg.*, 1992, **74A**, 233–238.

19 **Ahmed, A. M., Tissakht, M., Shrivastava, S. C.,** and **Chan, K.** Dynamic stress response of the implant/cement interface: an axisymmetric analysis of a knee tibial component. *J. Orthop. Res.*, 1990, **8**, 435–447.

20 **Hashemi, A.** and **Shirazi-Adl, A.** Finite element analysis of tibial implants – effect of fixation design and friction model. *Computer Meth. Biomech. Biomed. Engng*, 2000, **3**, 183–201.

21 **Shirazi-Adl, A.** and **Ahmed, A. M.** A parametric axisymmetric model study on the interface motions in porous-surfaced tibial implants. *Ann. Biomed. Engng*, 1989, **17**, 411–421.

22 **Rakotomanana, R. L., Leyvraz, P. F., Curnier, A., Heegaard, J. H.,** and **Rubin, P. J.** A finite element model for evaluation of tibial prosthesis–bone interface in total knee replacement. *J. Biomechanics*, 1992, **25**, 1413–1424.

23 **Walker, P. S., Greene, D., Reilly, D., Thatcher, J., Ben-Dov, M.,** and **Ewald, F. C.** Fixation of tibial components of knee prostheses. *J. Bone Jt Surg.*, 1981, **63A**, 258–267.

24 **Walker, P. S., Hsu, H. P.,** and **Zimmerman, R. A.** A comparative study of uncemented tibial components. *J. Arthroplasty*, 1990, **5**, 245–253.

25 **Shrivastava, S. C., Ahmed, A. M., Shirazi-Adl, A.,** and **Burke, D. L.** Effect of a cement–bone composite layer and prosthesis geometry on stresses in a prosthetically resurfaced tibia. *J. Biomed. Mater. Res.*, 1982, **16**, 929–949.

26 **Vasu, R., Carter, D. R., Schurman, D. J.,** and **Beaupre, G. S.** Epiphyseal-based designs for tibial plateau components. 1: stress analysis in the frontal plane. *J. Biomechanics*, 1986, **19**, 647–662.

27 **Ryd, L.** Micromotion in knee arthroplasty. A Roentgen stereophotogrammetric analysis of tibial component fixation. *Acta Orthop. Scand., Suppl.*, 1986, **220**, 1–80.

28 **Dammak, M., Shirazi-Adl, A., Schwartz Jr, M.,** and **Gustavson, L.** Friction properties at the bone-metal interface: comparison of four different porous metal surfaces. *J. Biomed. Mater. Res.*, 1997, **35**, 329–336.

29 **Cheal, E. J., Hayes, W. C., Lee, C. H., Snyder, B. D.,** and **Miller, J.** Stress analysis of a condylar knee tibial component: influence of metaphyseal shell properties and cement injection depth. *J. Orthop. Res.*, 1985, **3**, 424–434.

30 **Murase, K., Crowninshield, R. D., Pedersen, D. R.,** and **Chang, T. S.** An analysis of tibial component design in total knee arthroplasty. *J. Biomechanics*, 1983, **16**, 13–22.

31 **Askew, M. J.** and **Lewis, J. L.** Analysis of model variables and fixation post length effects on stresses around a prosthesis in the proximal tibia. *J. Biomech. Engng*, 1981, **103**, 239–245.

32 **Lewis, J. L., Askew, M. J.,** and **Jaycox, D. P.** A comparative evaluation of tibial component designs of total knee prostheses. *J. Bone. Jt Surg.*, 1982, **64A**, 129–135.

33 **Hvid, I., Jensen, J.,** and **Nielsen, S.** Contribution of the cortex to epiphyseal strength. The upper tibia studied in cadavers. *Acta Orthop. Scand.*, 1985, **56**, 256–259.

34 **Murray, R. P., Hayes, C. W., Edwards, W. T.,** and **Harry, J. D.** Mechanical properties of the subchondral plate and the metaphyseal shell. *Trans. Orthop. Res. Soc.*, 1984, 197.

35 **Bernakiewicz, M.** and **Viceconti, M.** The role of parameter identification in finite element contact analyses with reference to orthopaedic biomechanics applications. *J. Biomechanics*, 2002, **35**, 61–67.